

The study of scroll wave dynamics in personalized models of the left ventricle of the human heart

K. S. Ushenin^{*†‡} S. F. Pravdin^{*‡} Yu. S. Alueva[§] T. V. Chumarnaya^{*†}
and O. E. Solovyova^{*†‡}

Abstract — This paper presents first results on the dynamics of filaments of scroll waves of myocardium excitation obtained for personalized models of the left ventricle of the human heart. The paper describes a mathematical model of the left ventricle of the human heart and its electrical activity, numerical methods for the model calculation within the framework of computer implementation, and also the method of personalization of the model according to data of ultrasound examination. We found that regardless of the starting point of wave the filaments of wave drift along a spiral to the attractor located near the apex of the ventricle. The attractor position was essentially different in models constructed from the data of patients without identified pathology and those for patients with an increased left ventricular cavity.

Keywords: Spiral waves, drift of spiral waves, cardiac simulation, myocardium, personalized modeling.

MSC 2010: 92B99

Computer medicine is becoming now an integral part of modern medicine. The development of patient-oriented integrative mathematical and computational models of physiological systems for diagnostics, analysis of disease development scenarios, and choice of methods of their treatment is an independent, important, and urgent problem of personalized medicine.

It is known that cardio-vascular diseases are most common among socially significant diseases. Those are especially life-threatening and expensive to treat. Modern methods of diagnosis and visualization of the state of the cardiovascular system allow us to obtain data related to structural changes in the heart and vessels of patients with arrhythmias and heart failure, valvular and vascular diseases. These data can be used as input parameters for construction of personalized morphofunctional models of the heart used to detect possible violations of electrical and mechanical functions of the heart, prognosis of disease development and testing the methods of

*Ural Federal University, Ekaterinburg 620002, Russia. E-mail: kostanew@gmail.com

†Institute of Immunology and Physiology, Ural Branch of the RAS, Ekaterinburg 620049, Russia

‡Institute of Mathematics and Mechanics, Ural Branch of the RAS, Ekaterinburg 620990, Russia

§Sverdlovsk Regional Clinical Hospital No. 1, Ekaterinburg 620102, Russia

The work was supported by the Russian Science Foundation (project No. 14-35-00005, ‘Personalized models in cardiology’)

its treatment. In future, such model could be a powerful tool for making informed decisions by a doctor in the treatment of a particular patient taking into account factors usually ignored in traditional medical examinations where the individual characteristics of the patient are neutralized by statistical data processing.

In this paper we demonstrate the approach to construction of personalized models of the left ventricle (LV) of the human heart on the basis of individual images of the heart obtained in the clinic by echocardiography methods (ultrasound), magnetic resonance imaging (MRI), or computed tomography (CT). The specific feature of our method is the use of an analytical description of LV geometry and architecture of its myocardial fibres within the thickness of the wall developed by the authors in the previous work [10]. The use of analytical models of LV geometry allows us to construct personalized models even on the base of ultrasound data, which, on the one hand, are obtained by the most routine non-invasive and widely available method, and, on the other hand, are most noisy and insufficiently detailed.

The pilot results of functional modelling the activity of LV within the framework of personalized models are demonstrated on the example of the study of scroll wave dynamics imitating abnormal excitation of the left ventricle accompanied by a significant increase in the heartbeat frequency, i.e., ventricular tachycardia, due to a spontaneous periodic activation of LV.

In our previous papers we studied the drift of scroll waves in an idealized axisymmetric model of the left ventricle [12]. One of characteristics of a scroll wave is a filament, i.e., the curve around which the scroll wave spins. It was found that the scroll wave filament, as a rule, is slowly drifting in the thickness of LV wall up to reaching the attractor which is a three-dimensional ring parallel to the plane of the ventricle base. The filament is slowly moving in the side direction. It is known that the geometry and anisotropy of the medium can provide some impact on the drift of the scroll wave [2, 4].

Based on experience from the previous studies, we assumed that the drift of the filament in a non-axisymmetric personalized model of LV anatomy may occur in a more complex manner than in idealized symmetric models. In this paper we describe the approach applied to modelling LV electrophysiology within the framework of personalized anatomical models and pilot results on the dynamics of filaments of scroll waves.

1. Methods

In order to construct a personalized model of LV electrophysiology, we need an anatomical model describing the geometry of LV and architecture of myocardium fibres, a system of equations describing the propagation of the action potential (AP) in the myocardium, a computational method for its implementation, and an approach to personalization of the model according to data of medical diagnostics. In order to carry out effective computational experiments with the model, the used methods have to be implemented in a high-performance software.

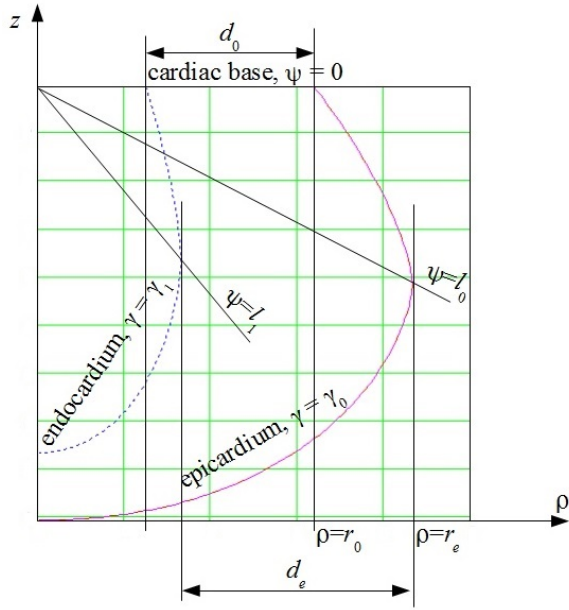


Figure 1. Meridional section of LV model [8].

1.1. Anatomical model

The model of LV architecture was developed in our group previously [8, 10]. It allows us to approximate the real shape of LV, specify the direction of fibres at each point of the geometric body, and use the model coordinate system for construction of a structured grid. The verification of the model was carried out on modern data of diffusion-tensor magnetic resonance imaging (DT-MRI) in [8].

The shape of LV is given by a mapping of special coordinates of the calculation domain (γ, ψ, φ) to the cylindrical coordinates (ρ, φ, z) of the physical space (Fig. 1). The coordinate $\gamma \in [\gamma_0, \gamma_1]$ specifies the position of a point in the thickness of the wall, i.e., $\gamma = \gamma_0$ on the subepicardial surface, $\gamma = \gamma_1$ on the subendocardial surface. The coordinate $\psi \in [0, \pi/2]$ specifies the position of a point relative to the apex and base (analogue of latitude), i.e., $\psi = 0$ for the base, $\psi = \pi/2$ for the apex. The coordinate $\varphi \in [0, 2\pi]$ is an analogue of longitude.

In some meridional sections that can be constructed on the base of clinical data the form of LV wall is determined by the following parameters: $r_{0,e}(\varphi)$ is the radius of LV on the epicardium base or equator; $l_{0,1}(\varphi)$ is the latitude of ψ on the equator of the epicardium or endocardium; $p(\varphi) > 1$ is the parameter specifying the curvature of the wall. The following parameters do not depend on the coordinate φ : the height Z of LV, the wall thickness h of LV on the apex.

The model of architecture of the myocardium used in the study is based on the ideas of Torrent-Guasp [18] and Streeter [15] about the patterns of fibre directions in the ventricular myocardium. Fibres lie on spiral surfaces nested one within the other and forming the thickness of the LV wall (Fig. 2). In special coordinates the

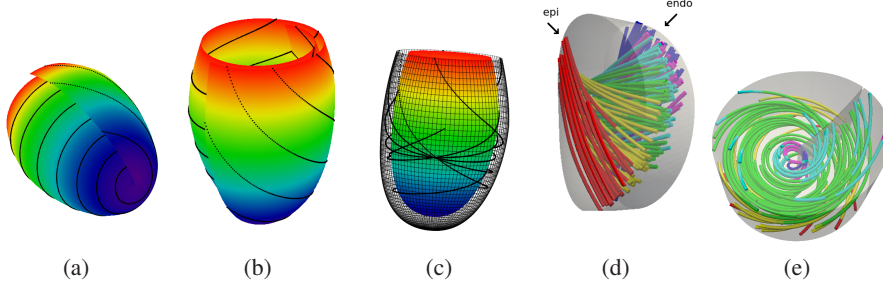


Figure 2. The model of LV constructed on the basis of heart ultrasound (see Fig. 4 below, model No. 5, the parameters $\gamma_0 = 0.1$, $\gamma_1 = 0.85$). Panels (a) and (b) show a certain spiral surface in the thickness of LV and the pattern of fibres in it. Panel (c) shows several fibres passing through a segment of transmural crossing of the wall in the middle part of the ventricle. The panels (d) and (e) visualize the transmural rotation of fibres in the LV wall. A ‘Japanese fan’ of fibre directions is shown (d) in the basal part of LV at the latitude level $\psi = \pi/8$ with the transmural angle $\Delta\alpha_1 \approx 135^\circ$ of rotation of fibres. Near the apex the fibres are placed mainly circularly (e), spin around the axis and pass through the wall with a lesser angle of transmural rotation ($\Delta\alpha_1 \approx 80^\circ$ on the latitude level $\psi = (7\pi/16)$). At the center of the apex the fibres are directed practically vertically.

spiral surface equation has the form

$$\varphi(\gamma, \varphi_{\min}, \varphi_{\max}) = \varphi_{\min} + \gamma\varphi_{\max}$$

where φ_{\max} is the rotation angle of the spiral surface (it is the same for all spiral surfaces). Different spiral surfaces forming the thickness of LV walls are specified by variation of the angle $\varphi_{\min} \in [0, 2\pi)$.

In this model the myocardium of LV consists of fibres lying on spiral surfaces forming the thickness of the wall.

Introduce notations for the polar system of coordinates $(P; \Phi)$, where P and Φ are the radial and angular coordinates, respectively. Myocardium fibres are constructed in the model as images of chords $Y = \text{const}$; $Y \in [0, 1)$ of the semicircle $P = 1$, $\Phi \in [0, \pi]$ parallel to its diameter on a fixed spiral surface. Each particular chord is parameterized by the polar angle $\Phi \in [\Phi_0, \Phi_1]$, where $\Phi = \arcsin Y$, $\Phi_1 = \pi - \arcsin Y$. The mapping of a point $(P; \Phi)$ on a chord to a point on a spiral surface is given by the formulas

$$\gamma(\Phi) = \frac{\Phi}{\pi}, \quad \psi(P) = (1 - P)\frac{\pi}{2}.$$

For example, the image of the diameter of the semicircle is the fibre beginning on the subepicardium, descending to the zone of the apex ($\psi = \pi/2$), and then rising up again to the base and ending on the endocardium. Images of shorter chords are closer to the base of LV and have lesser length. An example of an LV model with several fibres is presented in Fig. 2.

Fibres in the model begin at the subendocardium layer of the wall, go through the thickness of wall in the direction from the base to the apex, and end on the subepicardial layer. Drawing the transmural line connecting the endocardium and

the epicardium in an arbitrary region of the LV wall, the tangents to fibres are rotated relative to this line by some angle forming, as was noted by D. Streeter, some kind of a ‘Japanese fan’ [15] (Fig. 2d). This angle is called the *rotation angle of fibres* and is an important characteristic of the ventricle model (following [11], we denote it by $\Delta\alpha_1$). It was shown in several papers that the rotation angle of fibres in the wall of human LV is approximately equal to 135° [5, 15]. According to modern experimental data, the rotation angle of fibres is a variable value highly dependent on the type of animal, for example, for the dog it equals 145° , for the pig it approaches 180° [13]. Data for human LV were presented in [17], which gives the mean of 196.2° and the standard deviation of 73.2° .

Within the framework of our anatomical model, the rotation angle of fibres $\Delta\alpha_1$ is determined by the parameters $\gamma_0 \in [0, 1]$, $\gamma_1 \in [0, 1]$, $\gamma_0 < \gamma_1$ (see [8, 10]). The reduction of $\gamma_1 - \gamma_0$ causes a decrease in $\Delta\alpha_1$. The maximal value of $\gamma_1 - \gamma_0 = 1 - 0 = 1$ corresponds to the model with the largest rotation angle of fibres equal to 180° . The construction of an asymmetric LV model of the human heart on the basis of DT-MRI data [8] showed that the best approximation of direction of fibres in the thickness of the wall is attained for the values of parameters $\gamma_0 = 0.05$, $\gamma_1 = 0.98$. These values were used to construct personalized LV models. In this case the range of values of the rotation angle of fibres $\Delta\alpha_1$ in the basal region of LV is from 162° to 167° for different models (see Table 1), which falls within the range of observed values from [17]. In addition, we have taken such values of the model parameters $\gamma_0 = 0.1$, $\gamma_1 = 0.85$ when the rotation angle of fibres $\Delta\alpha_1$ in our personalized models was close to 135° [15]. The calculations were done for models with both sets of parameters γ_0 , γ_1 , and the results were qualitatively similar (see Section 3 below).

Using several meridional sections of the models constructed on these formulas, we have to reconstruct the three-dimensional LV geometry. It can be done by interpolation of each of the seven model parameters ($d_0, d_e, r_0, r_e, l_0, l_1, p$) between the sections using periodic cubic splines with respect to the coordinate φ . A personalized model of LV geometry can be constructed on the base of 4 and more meridional sections. In this paper we used 4 sections of LV obtained according to the data of echocardiographic examination (ultrasound) of the heart.

The main advantage of our approach to modelling the architecture of LV is the possibility of continuous variation of parameters and specification of the direction of fibres based on geometrical characteristics of LV and two variable parameters γ_0, γ_1 .

1.2. Electrophysiological model

In order to calculate the electrical activity of LV, in this paper we used the following mono-domain description of the three-dimensional myocardial tissue on the base of

phenomenological model of the myocardium of Aliev–Panfilov [1]:

$$\begin{aligned}\dot{u} &= -ku(u-a)(u-1) - uv + \nabla \cdot (D\nabla u) \\ \dot{v} &= \eta(u)(8u-v) \\ \eta(u) &= \begin{cases} 0.1, & u < a \\ 1, & u \geq a \end{cases}\end{aligned}$$

where variable u describes the variation of the membrane potential in the myocardium and variable v is a dimensionless characteristic of conductivity of the cell membrane for transmembrane ion currents.

The simulation of the anisotropy of the myocardial medium relative to the behaviour of the electric signal uses a uni-axial diffusion tensor D with the ratio of 9 to 1 for diffusion coefficients along and across the fibres of the myocardium. Due to this fact, the speed of excitation wave propagation in the myocardial tissue is 3 times greater along the fibres than across, which corresponds to experimental data. The values of the model parameters $k = 8$, $a = 0.03$ were fixed for all experiments described below.

The boundary condition of the electrodiffusion problem is that the electric current through the boundary of the calculation domain equals zero. The initial conditions providing the appearance of a scroll wave of excitation in the myocardium are described below in Section 1.5.

1.3. Numerical method

The problem of electrodiffusion is calculated with the use of the finite difference method (FDM) applied to the grid model of LV constructed in special coordinates (γ, ψ, φ) . The size of the grid is determined for each anatomical model separately and is transformed to physical coordinates by the mapping described in Subsection 1.1. Some nodes of the uniform grid are excluded because this grid is rather nonuniform in the physical space. The difference scheme for calculation of the reaction-diffusion equation with the use of Euler's method for ODE and also the methodology of construction and sparsening the grid were described in more detail in [9, 11].

The model of Aliev–Panfilov uses a dimensionless time variable, in this paper the unit of model time is taken equal to 36 ms. In this case the duration of the action potential (AP) generated by one cell in the model is equal to 290 ms, which is in accordance with the normal duration of AP in cells of human ventricle. The solution of the problem was performed with the time step $dt = 0.00166$ of model time and with a spatial step not exceeding 1 mm in the physical space.

1.4. Implementation of the model

The calculation software was implemented in C language (C99) with the use of OpenMP technology and Intel Composer 2015. The Python language was used for

the processing of results of numerical simulation. The ParaView package and the matplotlib module of Python were used for data visualization. The technical implementation of the project is described in more detail in [14].

1.5. Protocol of computational experiments

The initiation of the excitation scroll wave was done by specification of two adjacent domains of LV with different values of the membrane potential and conductivity, i.e., the domain of initial excitation with values of membrane potential exceeding the threshold level of initiation of AP ($u = 1, v = 0$) and the domain with the initial block of conduction, i.e., with a low conductivity of the medium ($u = 0, v = k$). Other domains of LV have initial conditions providing a normal conduction of the excitation ($u = 0, v = 0$). The domains of initialization of the wave were placed longitudinally from the base of LV to a given height in the direction to the apex, which determines the initial zone of scroll wave filament formation either in the middle part of the LV wall (latitude $\psi = 0.2\pi$), or closer to the apex ($\psi = 0.4\pi$). In this case the zones of initial activation were placed at one of six different meridians positioned at the angular distance $\pi/3$ from each other. The calculations were performed for not less than 20 seconds relative to units of model time.

2. Personalization of the model on the basis of clinical data

An important characteristic of the LV anatomy model is the number of its degrees of freedom in the case of LV approximation. Our model can be constructed on the basis of several meridional sections where the following parameters are specified:

- the radius r_0 from the axis to the epicardium and the LV wall thickness d_0 on the base;
- the radius r_e from the axis to the epicardium and the LV wall thickness d_e on the equator;
- the latitude ψ of the equator on the epicardium l_0 and endocardium l_1 ;
- the parameter p characterizing the curvature of the contour of LV.

The common parameters for all sections are the height Z of the longitudinal axis and the width h of the LV apex. In each cross-section of the model, the outer LV contour is associated with the three parameters (r_0, r_e, l_0), the three parameters (d_0, d_e, l_1) are associated with the inner contour. The curvature parameter p relates to both contours of LV. For example, the model constructed on the basis of ultrasound data from 4 cross-sections has 30 degrees of freedom for description of LV geometry and the additional variability related to the position of the apex in the plane of LV base.

Anonymized clinical data for construction of personalized models of human cardiac left ventricle were provided by the Sverdlovsk regional clinical hospital No. 1,

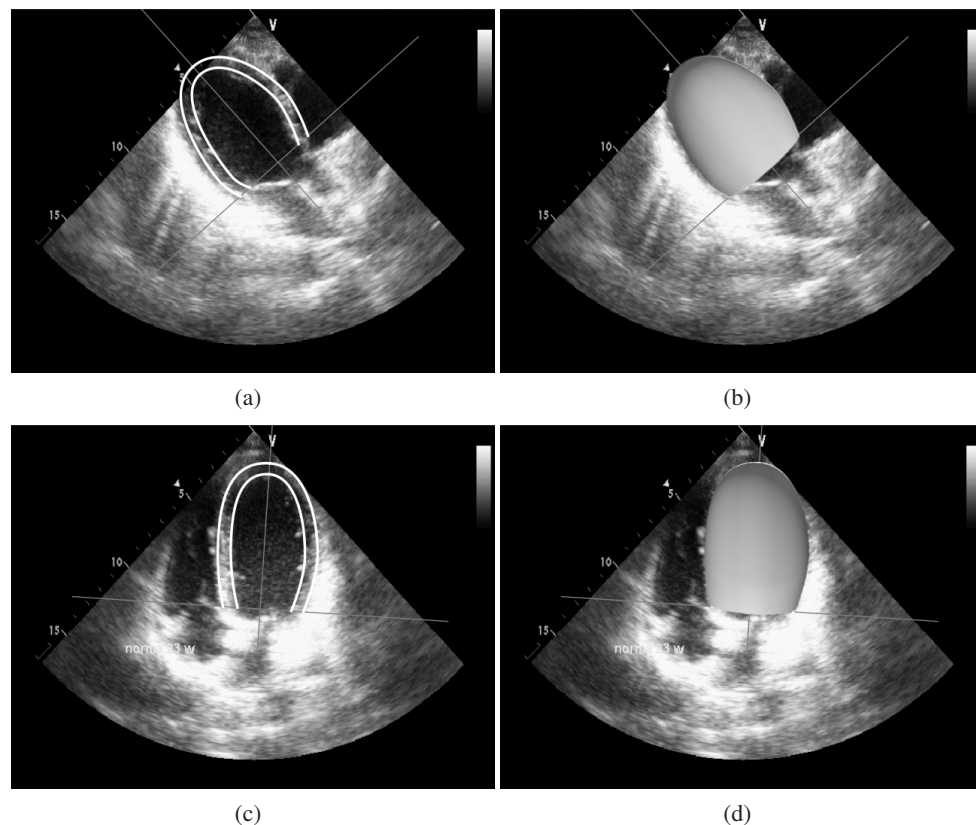


Figure 3. Echocardiographic image of the heart in the two-chamber and four-chamber positions with the superimposed pattern of the LV contour (a, c) and the three-dimensional anatomy model (b, d).

Ekaterinburg. The clinical data included the diagnosis of patients and the data of their echocardiographic examinations carried out on the unit of Phillips IE33 ultrasound system.

In order to construct personalized anatomical models of LV, we used echocardiographic images of LV in the end-diastole in the standard two- and four-chamber apical heart projections (Fig. 3). The construction of models was carried out by an expert specialist with the use of our software. The procedure of image processing consisted in overlaying a cross-section pattern of the anatomical model with the echocardiographic image on the screen of computer monitor and selection of the above model coefficients to achieve the best visual approximation of the epicardial and endocardial contours of the cross-section of LV model to the original projection image of LV. The procedure for selection of coefficients was repeated for each of the two halves of the LV image relative to a given axis for two ultrasound positions of the heart (Fig. 3). After processing LV cross-sections, the parameters Z and h of the model were averaged over all measured sections. This procedure took from 3 to 7 minutes for each ultrasound position of LV. Further, the software automatically ap-

plied the interpolation by cubic splines on the angle φ for each model parameter to obtain a three-dimensional body and calculated the direction of fibres as described above (see also [8]).

This method of constructing models of LV was previously verified against the data of DT-MRI in [8] for human and canine hearts, as well as in [6] for the human heart. The model showed a good approximation of the LV wall and direction vector of fibres in most regions of the wall. It was also shown in [6] that the mean value of the angle between fibre directions in the model and in experimental data is equal to 25° and this value practically does not increase with decreasing the number of projections of LV involved in the construction of the model from eight to four.

A significant limitation of the approach used in this paper is the visual expert assessment of the quality of approximation of echocardiographic data by the model. This approach is less complex in implementation compared to the known automatic methods of determination of image boundaries, but errors of the expert may affect the simulation results. In further work we plan to study the sensitivity of the model and the variability of results depending on the peculiarities of image processing.

The pilot simulation results for the electrical activity of the myocardium in personalized LV models presented in this paper were obtained based on images of LV for five patients without identified heart pathologies and also for patients with the diagnosis of dilated cardiomyopathy (DCMP) and ischemic heart disease (IHD) with the syndrome of weakness of sinus node. The geometrical parameters of LV of these patients are presented in Table 1. The patients with pathologies present a significant increase in linear dimensions and end-diastolic volume of LV. In addition, in the case of myocardial pathologies the shape of LV often becomes more rounded and the sphericity index (the ratio of lengths of the short and long axes) increases, which, for example, is observed for the patient No. 7 with IHD. The patient No. 6 with DCMP has the ratio of thickness of LV wall at the apex to the wall thickness at the middle or basal levels significantly less compared with other patients. The values of LV shape parameters in the personalized anatomical models are presented in Tables 1 and 2. A comparative view of longitudinal sections of these models is presented in Fig. 4.

3. Results

According to the protocol of computational experiments described above, we carried out two series of experiments with different parameters determining the rotation angle of fibres in the LV wall (see Section 1.1). Each series consisted of 84 experiments, namely, 12 experiments with different zones of the wave initiation for each of 7 presented anatomical models. The first series of experiments (see rows I in Table 1) was performed for the models constructed with the parameters $\gamma_0 = 0.05$, $\gamma_1 = 0.98$ taken from [8]. For these models the rotation angle of fibres in the basal part of the ventricle (for $\psi = \pi/8$) is equal to 165° in average. The second series of experiments (see rows II in Table 1) was performed for the models constructed with the parameters $\gamma_0 = 0.1$, $\gamma_1 = 0.85$ and in this case the rotation angle of fibres in the

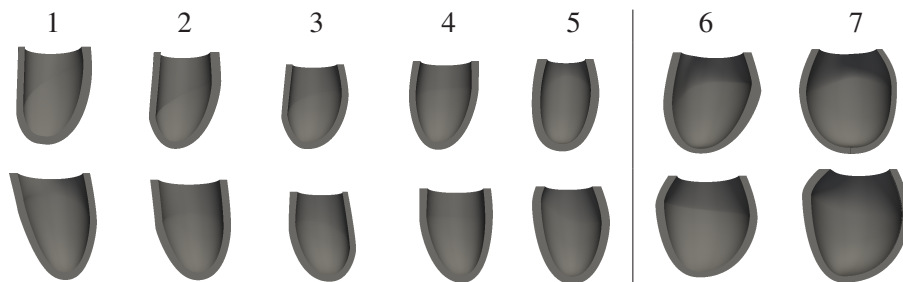


Figure 4. Cross-sections constructed for personalized models. Top row represents cross-sections of LV model corresponding to the image of four-chamber position. Bottom row represents cross-sections of the model for two-chamber position. Patients 1–5 are without detected pathologies. Patient 6 has the diagnosis of dilated cardiomyopathy. Patient 7 has the diagnosis of ischemic heart disease with the syndrome of weakness of sinus node.

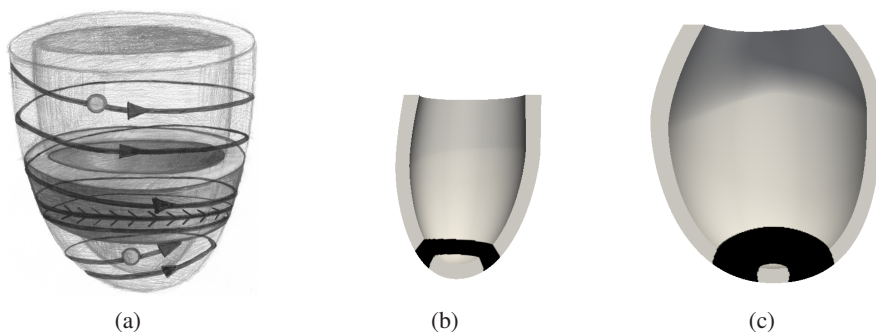


Figure 5. Illustration of the concept of wave drift to attractor (a). Lines indicate movement paths, the ring corresponds to the domain of attractor, circles show possible domains of wave initiation. The domain of circular attractor of the excitation scroll wave obtained in computational experiments is shown for model No. 4 of LV with the normal geometry (b) and for pathologically changed geometry No. 7 (c). The scale in subfigures (b) and (c) is coordinated.

basal part of the ventricle is 135° in average, which is closer to data from [15] for the human LV. In Tables 1 and 2 below we present all the parameters and characteristics of the constructed LV models and also the results of numerical experiments obtained for those values of the parameters γ_0, γ_1 . We note that in all considered personalized models the rotation angle of fibres fall into the range of experimentally observed values [17].

For all considered personalized models with a normal and abnormal LV geometry, and also for all methods of initiation of the scroll wave, we observed a drift of the wave filament in the direction of the attractor which settles in a region close to the apex of LV (see the scheme of wave drift in Fig. 5a). The attractor was a three-dimensional ring (see examples in Figs. 5a, 5b, and 5c) with the minimal and maximal values of ψ presented in Table 1 (recall that in the apex region coordinate ψ is close to 90°). After reaching the attractor, the filament continues its slow drift around the axis of LV.

The position (latitude ψ) of the middle line of the scroll wave filament attractor

Table 1. Geometrical characteristics of LV shape registered from echocardiographic images; parameters of the personalized model and parameters of attractors of scroll wave filaments. The index of sphericity is the indicator of LV shape defined as the ratio of the short ventricular axis to the long one. Parameters of the architecture of personalized anatomic models are the following: h is the wall thickness near the apex, \bar{d} and $\Delta\alpha_I^0$ are the mean wall thickness and the rotation angle of fibres in the basal part of LV. The minimal and maximal values of ψ° characterize the position of the attractor. The minimal distance from the filament to the middle of LV apex is indicated in degrees in the coordinate ψ and in mm. The series of experiments with different parameters of fibre orientations are denoted by Roman numbers I, II. I: $\gamma_0 = 0.05, \gamma_1 = 0.98$. II: $\gamma_0 = 0.1, \gamma_1 = 0.85$.

No.	Diagnosis	Geometric characteristics of LV obtained from ultrasound images			Parameters of the model				Parameters of the attractor of the filament to the apex		Minimal distance		
		Long axis (mm)	Short axis (mm)	Index of sphericity	End-diastole volume (ml)	h (mm)	\bar{d} (mm)	ser.	$\Delta\alpha_I^0$	Min. ψ°		Max. ψ°	($^\circ$)
1	Normal	65	33	0.486	151	5.40	6.8	I	167	53.9	62.7	27.3	14.3
								II	147	63.9	71.1	18.9	9.2
2	Normal	76	39	0.514	128	5.34	7.7	I	167	56.1	73.3	16.7	14.3
								II	147	66.3	73.9	16.1	8.2
3	Normal	62	40	0.652	96	5.02	6.4	I	167	59.9	67.8	22.2	14.7
								II	138	63.5	70.5	19.5	10.2
4	Normal	64	40	0.638	106	5.45	6.5	I	166	47.1	62.4	27.6	17.2
								II	134	57.5	67.5	22.5	11.5
5	Normal	72	40	0.545	100	5.73	6.7	I	166	57.5	67.1	22.9	13.6
								II	137	66.5	73.4	16.6	9.1
6	DCMP	84	52	0.628	194	4.38	10.7	I	162	73	80.5	9.5	7.9
								II	129	70	82.1	7.9	6.5
7	IHD	93	75	0.812	254	5.50	6.5	I	163	64.8	79.7	10.3	7.7
								II	130	69.2	82.4	7.6	6.1

Table 2.

Complete list of parameters of personalized anatomic models used in the study. Parameters for series I and II are separated by a vertical line.

No.	Common parameters	No. of section	r_0 (mm)	r_e (mm)	d_0 (mm)	d_e (mm)	l_0	l_e	p
1	$h = 5.4(\text{mm})$	1	14.8	21.6	6.1	5.8	0.572	0.638	1.414
	$Z = 84.55(\text{mm})$	2	38.3	41.1	8.5	7.5	0.227	0.195	1.878
	$\gamma_0 = 0.05 \mid 0.1$	3	43.2	36.2	6.5	4.5	0.410	0.358	1.039
	$\gamma_1 = 0.98 \mid 0.85$	4	14.3	20.2	8.1	7.3	0.755	0.839	1.652
2	$h = 5.34(\text{mm})$	1	20.3	24.1	6.1	5.8	0.546	0.612	1.679
	$Z = 79.18(\text{mm})$	2	35.9	38	7.8	7.7	0.299	0.338	1.585
	$\gamma_0 = 0.05 \mid 0.1$	3	35.7	31.7	6.1	5.3	0.540	0.527	1.136
	$\gamma_1 = 0.98 \mid 0.85$	4	13.6	20.0	7.3	5.9	0.742	0.833	1.359
3	$h = 5.02(\text{mm})$	1	6.9	15.7	5.8	5.2	0.813	0.904	1.370
	$Z = 69.44(\text{mm})$	2	32.8	37.4	5.4	5.7	0.312	0.325	1.765
	$\gamma_0 = 0.05 \mid 0.1$	3	32.5	32.1	6.1	5.0	0.403	0.351	1.468
	$\gamma_1 = 0.98 \mid 0.85$	4	12.2	17.8	6.5	5.3	0.742	0.813	1.250
4	$h = 5.45(\text{mm})$	1	19.3	21.1	5.9	6.0	0.253	0.358	1.954
	$Z = 71.66(\text{mm})$	2	34.8	34.2	6.4	5.8	0.291	0.310	1.484
	$\gamma_0 = 0.05 \mid 0.1$	3	33.5	33.2	6.2	5.2	0.334	0.306	1.401
	$\gamma_1 = 0.98 \mid 0.85$	4	17.3	21.8	6.5	5.6	0.439	0.468	1.756
5	$h = 5.73(\text{mm})$	1	21.3	28.0	6.7	6.2	0.377	0.415	1.650
	$Z = 72.72(\text{mm})$	2	24.0	28.7	6.6	6.7	0.377	0.377	1.690
	$\gamma_0 = 0.05 \mid 0.1$	3	26.9	29.7	6.9	6.6	0.181	0.172	1.710
	$\gamma_1 = 0.98 \mid 0.85$	4	19.9	24.5	7.9	6.8	0.506	0.535	2.163
6	$h = 4.38(\text{mm})$	1	45.7	56.8	6.5	6.2	0.403	0.429	1.785
	$Z = 95.15(\text{mm})$	2	51.9	60.2	7.9	9.7	0.403	0.306	1.203
	$\gamma_0 = 0.05 \mid 0.1$	3	20.7	35.3	10.2	7.6	0.227	0.253	1.757
	$\gamma_1 = 0.98 \mid 0.85$	4	21.5	30.3	9.3	9.6	0.612	0.612	1.675
7	$h = 5.46(\text{mm})$	1	45.7	56.8	6.5	6.2	0.403	0.429	1.785
	$Z = 97.59(\text{mm})$	2	25.9	40.8	6.9	5.4	0.358	0.390	2.171
	$\gamma_0 = 0.05 \mid 0.1$	3	20.7	35.3	10.2	7.6	0.227	0.253	1.757
	$\gamma_1 = 0.98 \mid 0.85$	4	34.0	46.5	7.8	6.8	0.384	0.436	1.718

is at a larger distance from the apex in LV models for patients without cardiac pathology in comparison to those with heart disease, see Fig. 5, and also the minimal distance from the filament to the apex in LV models in Table 1, for models with the normal geometry of LV the distance from the apex is greater than for LV models with a pathologically changed geometry. In this case the simulation results are not qualitatively different in both series of experiments, although in the models with large rotation angle of fibres for $\gamma_0 = 0.05$, $\gamma_1 = 0.98$ the attractors were located by 2–7 mm higher than in the models with $\gamma_0 = 0.1$, $\gamma_1 = 0.85$ (see the results for series I and II in Table 1).

It is interesting to note that from the viewpoint of the theory of spiral waves, in the isotropic case the scroll wave filament must drift to the domain with the smallest thickness of the excitable body [3, 19], i.e., in the models considered here to the region of LV apex. However, due to the anisotropy and a complex shape of the ventricle, the filament is settled in all models at some distance from the apex, and the distance was larger in models with a normal LV geometry.

It was also shown earlier on axisymmetric models that the position of the attractor may differ from predictions of the theory and can be settled even in the domain with a greater wall thickness depending on the ratio of wall thicknesses on the base and on the apex of the ventricle and on characteristics of its shape, for example, in the case of its greater sphericity [11]. In addition, it was shown that the drift of the filament can depend on the curvature of the LV wall and the anisotropy of the medium [4]. The pilot results obtained here require further more detailed analysis.

The architecture of fibres in the LV apex region is significantly more difficult than in the middle and basal areas of the wall. The DT-MRI data possess a big variability in directions of fibres, although the measurement error in this area can be relatively large. In our models the angle of transmural rotation of fibres near the apex ($\psi = 7\pi/16$) was about 60° in pathological cases and about 80° in normal ones, and a predominantly circular arrangement of fibres was observed, whereas just in the area of apex ($\psi > 87^\circ$) the fibres go almost perpendicular to the LV wall (see Fig. 2e). This behaviour of fibres can lead to a sharp curvature of the front of a scroll wave and even create preconditions for the wave break-up, which corresponds to a ventricle fibrillation in the real heart.

An unstable behaviour of the scroll wave was detected previously in axisymmetric models of LV for some geometrical parameters of LV and parameters of the cellular model contributing to the growth of the filament and its drift to the thickened apex of the heart [12]. Therefore, the settlement of a filament sufficiently close to the apex in LV models with a pathologically changed shape can contribute to an increased risk of fibrillation.

4. Conclusions

In this work we first used the method developed in our group for construction of personalized models of LV using its images obtained in echocardiographic examination. Our approach using the analytic model of the LV shape and directions of

fibres allows us to carry out a three-dimensional reconstruction of LV reflecting its individual characteristics even for small amount of information (only 2 flat meridional sections) and not very high quality of images obtained from echocardiographic images.

We do not describe here all possible peculiarities of behaviour of scroll waves on personalized models of LV with typical variations of its form observed in the case of some of other pathology. This is a subject of further statistical analysis requiring data processing on representative groups of patients with different types of geometrical and functional LV remodelling, as well as calculations using different protocols. In addition, we also plan to conduct a study of the dynamics of scroll waves using personalized models of LV geometry and more detailed ionic models of cellular activity (see, e.g., ten Tusscher et al. [16] and the Ekaterinburg–Oxford [7]).

Thus, in this paper we have found that the dynamics of scroll waves within personalized LV models is sensitive to peculiarities of the individual heart geometry. An enlargement of the LV cavity volume is typical for heart diseases as well as a change in the ratio of wall thicknesses at the base and apex, the curvature of the wall, and sphericity of LV shape, and also the rotation angle of fibres in different regions of the wall, especially near the apex. Such remodelling of LV can generate its substrate independent of other factors increasing the probability of arrhythmias.

Acknowledgements

The authors are grateful to A. V. Panfilov and L. B. Katsnelson for helpful comments in the course of the work and useful discussion of its results. The calculations were performed on the ‘Uran’ cluster of the Ural Branch of the Russian Academy of Sciences.

References

1. R. R. Aliev and A. V. Panfilov, A simple two-variable model of cardiac excitation. *Chaos, Solitons and Fractals* **7** (1996), No. 3, 293–301.
2. I. V. Biktasheva, H. Dierckx, and V. N. Biktashev. Drift of scroll waves in thin layers caused by thickness features: Asymptotic theory and numerical simulations. *Phys. Rev. Letters* **114** (2015), No. 6, 1–5.
3. V. N. Biktashev, A. V. Holden, and H Zhang, Tension of organizing filaments of scroll waves. *Philos. Trans. Royal Soc. London A: Math. Phys. Engrg. Sci.* **347** (1994), No. 1685, 611–630.
4. H. Dierckx, E. Brisard, H. Verschelde, and A. V. Panfilov, Drift laws for spiral waves on curved anisotropic surfaces. *Phys. Review E - Statistical, Nonlinear, and Soft Matter Physics* **88** (2013), No. 1.
5. R. A. Greenbaum, S. Yen Ho, D. G. Gibson, A. E. Becker, and R. H. Anderson, Left ventricular fibre architecture in man. *British Heart J.* **45** (1981), No. 3, 248–263.
6. A. A. Koshelev, S. F. Pravdin, K. C. Ushenin, A. E. Bazhutina, L. B. Katsnelson, and O. E. Solovyova, Modified mathematical model of the cardiac left ventricle anatomy. *Biofizika* (2016) (in Russian) (in print).
7. V. S. Markhasin, O. Solovyova, L. B. Katsnelson, Yu. Protsenko, P. Kohl, and D. Noble,

- Mechano-electric interactions in heterogeneous myocardium: Development of fundamental experimental and theoretical models. *Progress Biophys. Molecular Biology*, **82** (2003), No. 1–3, 207–220.
8. S. F. Pravdin, Nonaxisymmetric mathematical model of the cardiac left ventricle anatomy. *Russ. J. Biomech.* **17** (2013), No. 4(62), 75–94.
 9. S. F. Pravdin, A method of solving reaction-diffusion problem on a non-symmetrical model of the cardiac left ventricle. In: *Proc. 47th Int. Youth School-Conference 'Modern Problems in Mathematics and its Applications'*. Ekaterinburg, Russia. IMM UB RAS, Ekaterinburg, 2016, pp. 284–296.
 10. S. F. Pravdin, V. I. Berdyshev, A. V. Panfilov, L. B. Katsnelson, O. Solovyova, and V. S. Markhasin, Mathematical model of the anatomy and fibre orientation field of the left ventricle of the heart. *Biomed. Engrg. Online* **12** (2013), No. 54.
 11. S. F. Pravdin, H. Dierckx, L. B. Katsnelson, O. Solovyova, V. S. Markhasin, and A. V. Panfilov, Electrical wave propagation in an anisotropic model of the left ventricle based on analytical description of cardiac architecture. *PLoS ONE* **9** (2014), No. 5.
 12. S. Pravdin, H. Dierckx, V. S. Markhasin, and A. Panfilov, Drift of scroll wave filaments in an anisotropic model of the left ventricle of the human heart. *Biomed. Res. Int.* (2015), 389830.
 13. R. M. Smith, A. Matiukas, C. W. Zemlin, and A. M. Pertsov, Nondestructive optical determination of fibre organization in intact myocardial wall. *Microscopy Research and Technique* **71** (2008), No. 7, 510–516.
 14. A. V. Sozykin, S. F. Pravdin, A. V. Koshelev, V. S. Zverev, K. S. Ushenin, and O. Solovyova, Leven — a parallel system for simulation of the heart left ventricle. In: *Application of Information and Communication Technologies (AICT), 2015 9th International Conference on 2015*, IEEE, Rostov-on-Don, pp. 249–252.
 15. D. D. Streeter, Gross morphology and fiber geometry of the heart. In: *Handbook of Physiology*, American Physiolog. Soc., Bethesda, 1979, pp. 61–112.
 16. K. H. W. J. Ten Tusscher, D. Noble, P. J. Noble, and A. V. Panfilov, A model for human ventricular tissue. *Amer. J. Physiol. Heart Circul. Physiol.* **286** (2004), H1573–H1589.
 17. J. M. Tigar, *3D Analysis of the Myocardial Microstructure: Determination of Fiber and Sheet Orientations*. BestMasters. Springer, Fachmedien Wiesbaden, 2015.
 18. F. Torrent-Guasp, *The Cardiac Muscle*. Guadarrama, Madrid, 1973.
 19. H. Verschelde, H. Dierckx, and O. Bernus, Covariant stringlike dynamics of scroll wave filaments in anisotropic cardiac tissue. *Phys. Rev. Lett.* **99** (2007), No. 16.